J. Phys. B: Atom. Molec. Phys., Vol. 9, No. 8, 1976. Printed in Great Britain.

The scattering of electrons by potassium atoms

D L Moores

Department of Physics and Astronomy, University College London, Gower Street, London WC1E 6BT, England

Received 3 December 1975

Abstract. A three-state (4s–4p–3d) close-coupling approximation is applied to the scattering of electrons with energies of up to 5 eV by potassium atoms. Amplitudes for elastic scattering and 4s → 4p excitation have been computed and this data stored in the British Library. Good agreement with the behaviour of the elastic differential cross section at fixed angle observed by Eyb and Hofmann in the immediate vicinity of the first excitation threshold is obtained. The threshold structure is analysed in detail.

For elastic scattering below the excitation threshold good agreement is obtained with the absolute differential measurements by Collins *et al* (1971) and by Slevin *et al* (1972) and the present results do not differ to any great extent from the calculations of Karule (1965, 1972) and Karule and Peterkop (1965). Above the excitation threshold and in its vicinity however, some differences between the calculations are apparent. Good agreement is obtained with the absolute elastic and inelastic angular distributions measured by Slevin *et al*, except for the case of elastic scattering at 3 eV, and also with the results of recoil experiments by Goldstein *et al* (1972). Total 4s → 4p excitation cross sections are in reasonable agreement with uncorrected data of Zapesochnyi and Shimon (1966). The total scattering cross sections are in less good agreement with the results of Visconti *et al* (1971) than are the calculations of Karule and Karule and Peterkop but still lie within the experimental uncertainties.

1. Introduction

In previous papers, results of calculations of cross sections and other related parameters for scattering of slow electrons by lithium and by sodium atoms (Norcross 1971, Moores and Norcross 1972), of cross sections for photodetachment of the alkali-metal negative ions (Moores and Norcross 1974) and of their electron affinities (Norcross 1974) have been reported. In all this work, the electron–atom problem was solved by the close-coupling method, with the target alkali-metal atom represented by a single valence electron moving in a central potential of scaled Thomas–Fermi form augmented by extra terms to allow for static dipole and quadrupole polarization of the closed-shell core plus non-adiabatic corrections to the dipole term. These potentials contained parameters which were adjusted in order to reproduce the observed separations of the first few target energy levels. In this paper, results obtained for the scattering of slow electrons by potassium atoms, using the same techniques, are reported. The theory has been adequately described in our previous publications and will not be repeated here. Previous close-coupling calculations by Karule (1965, 1972) (below the excitation threshold) and by Karule and Peterkop (1965) (above it) employed a two-state (4s–4p) expansion. Exchange was taken into account for the

first four partial waves, and a total of nine partial waves was included. The target wavefunctions were calculated using Gaspar's semi-empirical central potential (Gaspar 1952) which does not allow for core polarization. In the present study the effects of using our alternative target functions are investigated and the two-state close-coupling calculations extended by inclusion of the 3d state in the expansion.

Measurements of the differential elastic scattering cross sections as a function of energy, but at fixed angle, have been made by Eyb and Hofmann (1975) between 1 and 2 eV, that is, in the vicinity of the excitation threshold. The curves obtained are similar to the ones published for sodium by Andrick *et al* (1972) and show remarkable changes of shape as the angle of scattering is varied; what appears to

Table 1. Parameters used in semi-empirical model potential for K.

State	λ	r_c	ϵ (obs)†	ϵ (calc)
4s	0·99	2·2	0·319037	0·319042
4p	0·99	1·8677	0·200355	0·200357
5s	0·99	2·2	0·12743	0·12742
3d	0·99	2·7477	0·122787	0·122788
$\alpha_p = 5{\cdot}473$		$\alpha_q = 88{\cdot}0$	$\beta = 3{\cdot}843$	

† Since the theoretical model used neglects all spin orbit effects, the observed energies tabulated are statistically weighted mean values of the corresponding doublets.

be a sharp cusp being observed at about 1·61 eV between 100° and 120°, which vanishes near 60° and 135°. On the assumption that the feature observed is in fact the predicted Wigner cusp, and thus occurs exactly at the excitation threshold, it has been used for energy calibration purposes in experiments using the same apparatus for scattering of electrons by N_2 molecules. A second object of the present work is therefore to carry out a detailed study of the behaviour of the differential cross section over a small energy interval on either side of the threshold and to interpret any structure obtained. Thirdly, a variety of measured parameters has been calculated† over a range of energies between 0·5 and 5 eV and comparison made with a selection of other experimental and theoretical work.

2. Procedure

The parameters used to specify the semi-empirical model potential describing the interaction between external electrons and the K^+ core are given in table 1, together with the corresponding eigenenergies in rydbergs. This set was first obtained by Norcross (1974) for use in the electron-affinity calculations and subsequently employed by Moores and Norcross (1974) for the improved photodetachment calculations described on page 1656 of their paper. With this choice of parameters, the first excitation threshold is calculated to occur at 1·61477 eV.

† All necessary definitions are given in the paper on electron–sodium scattering (Moores and Norcross 1972).

Solution of the close-coupling equations yields a set of reactance matrix elements for each value of the total orbital angular momentum L and spin S. Once these data are given, any quantity connected with the scattering problem, measurable or otherwise, is readily computed, provided only that it does not depend upon phenomena neglected in the original problem, such as relativistic effects. Space considerations however preclude publication of reactance matrices, and the results have been presented in the form of tables of scattering amplitudes, this being considered the most useful scheme consistent with compactness. It is also possible that recently designed experimental arrangements such as those of Hertel and Stoll (1974) or Eminyan *et al* (1974) could enable direct measurements of the magnitudes and relative phases of these amplitudes to be made.

For elastic scattering the singlet and triplet amplitudes are given by (cf Moores and Norcross 1972, equation (2.7))

$$f^S(\theta) = \frac{\mathrm{i}}{2k_\mathrm{i}} \sum_{L=0}^{\infty} (2L + 1) P_L(\cos\theta) T^{S,L}_{4\mathrm{s}L,4\mathrm{s}L} \tag{2.1}$$

and for excitation of the 4p state we have

$$f^S_M(\theta, \phi) = \frac{1}{2\mathrm{i}} \left(\frac{4\pi}{k_\mathrm{i} k_\mathrm{f}}\right)^{1/2} \sum_{L, l_2 = L \pm 1} \mathrm{i}^{L - l_2} (2L + 1)^{1/2} C^{l_2 1 L}_{-M M 0} Y_{l_2}^{-M}(\theta, \phi) T^{S,L}_{4\mathrm{s}L,4\mathrm{p}l_2} \tag{2.2}$$

(Moores and Norcross 1972, equation (2.12)†). In (2.2) $S = 0$ or 1 and $M = \pm 1$ or 0.

The partial-wave expansions (2.1) and (2.2) of the scattering amplitude converge rather more slowly than do the corresponding expressions for cross sections and a large number of values of L must be included to attain reasonable accuracy. However, for the larger values of L simpler approximations are adequate; as L increases, first of all exchange may be neglected and eventually the Born approximation gives accurate reactance matrix elements. For elastic scattering, for large L (say $L > L_2$) one may use the expression

$$T^L_{4\mathrm{s}L,4\mathrm{s}L} = \frac{-2\pi\mathrm{i}\alpha k_\mathrm{i}^2}{(2L + 3)(4L^2 - 1)} \tag{2.3}$$

where α is the dipole polarizability, which we have taken to be equal to 300·0 atomic units. With this approximation, (2.1) may be summed to infinity to give

$$f^S(\theta) = \frac{\mathrm{i}}{2k_\mathrm{i}} \sum_{L=0}^{L_2} (2L + 1) T^{S,L}_{4\mathrm{s}L,4\mathrm{s}L} P_L(\cos\theta) + \pi\alpha k_\mathrm{i} \left(\frac{1}{3} - \frac{1}{2}\sin\frac{\theta}{2} - \sum_{L=1}^{L_2} \frac{P_L(\cos\theta)}{(2L + 2)(2L - 1)}\right). \tag{2.4}$$

For excitation, the Born integral expression, with the potential replaced by its asymptotic form (Seaton 1961) was used for the T-matrix elements for large values of

† Dr I Hertel has pointed out an error in this paper in the line following equation (2.12), the correct form of which should be 'For $M = 1$ we have $f^{\Xi}_1 = -f^{\Xi}_{\bar{1}}$'. This error, however, does not affect any of the curves or tabulated results since they all depend on the square of the absolute value of the amplitude.

Table 2. Ranges of L (the total angular momentum) for which various approximations were used to evaluate the T-matrix elements required in summing a partial wave expansion for the scattering amplitudes. (*a*) elastic scattering, (*b*) 4s→4p excitation where applicable.

E(eV)		Three-state	Three-state, no exchange	Two-state, no exchange	Born
0·5		0–3	4–8	—	⩾9
0·75		0–3	4–8	—	⩾9
1·0		0–3	4–8	—	⩾9
1·1		0–3	4	5–8	⩾9
1·2		0–3	4	5–8	⩾9
1·5		0–4	5–6	7–8	⩾9
1·6		0–3	4–5	6–8	⩾9
1·6131		0–3	—	4–8	⩾9
1·6140		0–3	—	4–8	⩾9
1·6155	(*a*)	0–3	—	4–8	⩾9
	(*b*)	0–3	—	—	4–9
1·6165	(*a*)	0–3	—	4–8	⩾9
	(*b*)	0–3	—	4	5–10
1·65	(*a*)	0–3	4	5–8	⩾9
	(*b*)	0–3	4	—	5–10
1·7	(*a*)	0–3	4–6	7–8	⩾9
	(*b*)	0–3	4–6	7–8	9–12
2·0	(*a*)	0–3	4	5–8	⩾9
	(*b*)	0–3	4	5–8	9–17
2·5	(*a*)	0–5	6–12	13–15	⩾16
	(*b*)	0–5	6–12	—	13–25
3·0	(*a*)	0–5	6–13	14–18	⩾19
	(*b*)	0–5	6–13	—	14–40
4·0	(*a*)	0–6	7–16	17–21	⩾22
	(*b*)	0–6	7–16	17–21	22–50
5·0	(*a*)	0–6	7–17	18–25	⩾26
	(*b*)	0–6	7–17	18–25	26–54

L, and the summation was terminated when neglected terms in (2.2) contributed less than 1%. The approximations adopted for different ranges of L are indicated in table 2. At energies very close to the excitation threshold, the three-state no-exchange calculation for $L \geqslant 4$ proved to be inaccurate (for numerical reasons) and the two-state results were used instead for these partial waves. The effect of doing this on amplitudes and cross sections was found to be insignificant.

For all the energies given in table 2, scattering amplitudes for excitation and elastic scattering were calculated, from equations (2.2) and (2.4), at 10° intervals over the range 0–180°. This data has been deposited with the British Library Supplementary Publications Scheme and is available on application to the British Library, Lending Division, Boston Spa, Wetherby, Yorkshire LS23 7BQ, quoting reference number SUP 70018.

In addition to the energies listed in table 2, differential cross sections were calculated at $\pm 9 \times 10^{-6}$ and $\pm 16 \times 10^{-6}$ Ryd from the excitation threshold. For these energies, it was only necessary to solve the coupled equations for the P waves (both of which have matrix elements T_{11} with discontinuous slope at threshold) and the ^{1}D partial wave which is not slowly varying owing to a resonance. For all other partial waves the T-matrix elements T_{11} were sufficiently slowly varying over this narrow energy range that they could be interpolated with sufficient accuracy.

3. Results

3.1. Elastic scattering phaseshifts

We first compare the results of a two-state (4s–4p) calculation with those of the similar calculation by Karule. Both the ^1S and ^3S two-state phaseshifts were found to be in excellent agreement with those obtained by Karule, and the ^3P phase in which a low-energy resonance is obtained, was also in good agreement. However, for the ^1P and both D waves, our phases were significantly larger, the discrepancy becoming greater with increasing energy above about 0·5 eV, while for $L > 2$ our phases were slightly larger than those of Karule. This situation is different from that existing for e^-–Na scattering (Moores and Norcross 1972) where our results were in excellent agreement with those of Karule for all partial waves. The main difference between the present calculations and those of Karule is the inclusion in our work of core polarization. This effect might be expected to be more important for K than for Na, and this could provide a possible explanation for the difference in the results.

If now the 3d state is added to the close-coupling expansion, the $^{1,3}S$ phases (and also those for $L > 2$) are scarcely changed, whereas the other partial waves are affected in different ways. The ^1P, ^1D and ^3D phases are illustrated in figure 1 and compared with the two-state results. The ^1P phase is decreased over the entire energy range except immediately below the 4p excitation threshold, where the sharp

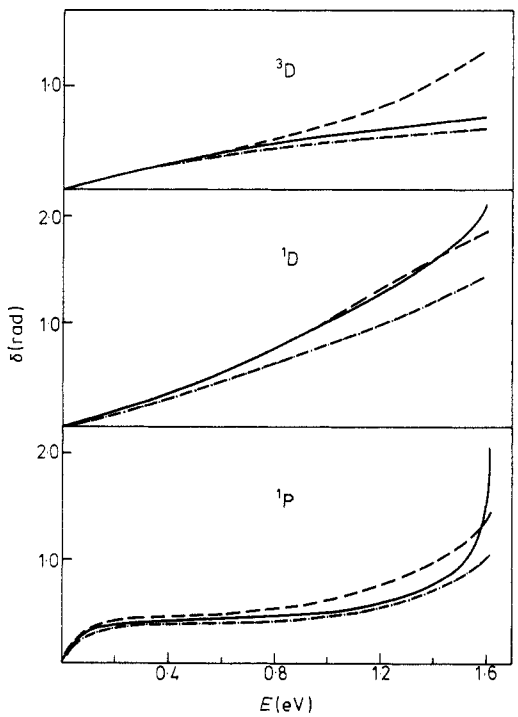

Figure 1. Phaseshifts for elastic scattering of electrons by potassium atoms. Karule (1965): chain curve; present results, two-state: broken curve and three-state, full curve.

narrow resonance responsible for the structure observed in the photodetachment of K^- (Moores and Norcross 1974) causes it to rise abruptly. The form of the two-state curve indicates the possible presence of a resonance somewhere above threshold. The ^1D phaseshift is increased above about 1·5 eV. This partial wave exhibits a very broad resonant behaviour, passing through $\pi/2$ at about 0·103 Ryd. The ^3D phaseshift is decreased to such an extent that the three-state value is in much better agreement with Karule's two-state value than with our own. The ^3P phase is only affected near the resonance, which is shifted to lower energy. This phaseshift goes through $\pi/2$ at about 0·02 eV, the corresponding partial cross section having a maximum value in excess of $6000\pi a_0^2$ ($5{\cdot}28 \times 10^{-13}$ cm^2) at this energy. The fact that some of the phaseshifts are found to decrease on inclusion of an additional closed channel in the close-coupling expansion is not consistent with the general principle discussed by a number of authors (e.g. Hahn *et al* 1964) that the phaseshift must necessarily increase under such circumstances. However, it may be shown that the conditions required for the validity of this principle are not satisfied when semi-empirical wavefunctions and potentials of the form employed in the present work are used to describe the target atom. On the other hand, the resonances which occur are shifted to lower energy by inclusion of the 3d state. The phaseshifts calculated by Sinfailam and Nesbet (1973) are in reasonable agreement with the present results, although they tend to be a bit lower away from the excitation threshold. On the whole, there is no major discrepancy between any of the calculations except in the neighbourhood of resonances.

3.2. Threshold effects

Assuming short-range forces and a constant M matrix, theory predicts that for the P waves near the excitation threshold, the elastic T-matrix element, T_{11}, should behave like

$$T_{11} = T_{11}(0) + A\sqrt{E_2} \tag{3.1}$$

where E_2 is the energy with respect to the excited state (below threshold E_2 is negative and $\sqrt{E_2}$ imaginary) and A is a complex constant. This leads to a discontinuous derivative in the partial cross section. An improved numerical technique, which ensures good linear independence of the wavefunctions in the asymptotic region, has been developed by Norcross and Seaton (1973) to enable calculations to be made much closer to thresholds than was formerly possible. Making use of this technique, T matrices were obtained to within $\pm 9 \times 10^{-6}$ Ryd of threshold. However even over this small range of energy the computed T_{11} for P-wave scattering could not be fitted to an expression of the form (3.1), owing to rapid variation of the M-matrix elements; though in the ^3P case the terms responsible only contributed to the third significant figure, so that the effect was scarcely detectable. To within the precision of the calculation, all other partial wave T matrices varied smoothly through threshold.

4. Comparison with experiment

4.1. Differential cross sections near the inelastic threshold

In the experiment of Eyb and Hofmann the differential cross section $\sigma(\theta)$ is found to undergo striking changes in its variation with energy near 1·6148 eV as the angle

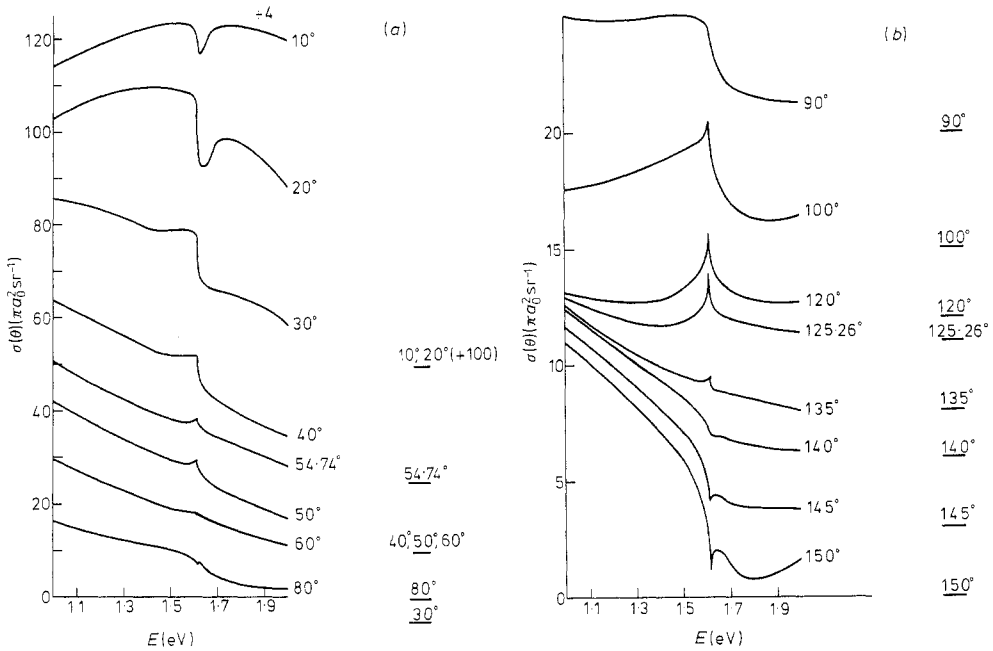

Figure 2. Differential cross sections (at fixed angle) as a function of energy, between 1 and 2 eV. The scale on the left-hand side is in units of $\pi a_0^2\,\mathrm{sr}^{-1}$; the zero point corresponding to each angle is marked on the right.

of scattering is varied. Below 60° the cross section decreases with energy with some evidence of an abrupt drop at threshold, followed by a shallow dip; at 60° the threshold effect appears to vanish and a smooth curve is obtained. Towards 90° a steplike feature appears to develop near the threshold, while between 100° and 130° a sharp upward peak is observed. Around 135° the curve flattens out and becomes monotonically decreasing, with no structure, while for larger angles there is a tendency for a dip to appear just above threshold and the variation with energy is similar to that observed at small angles.

With some minor differences, and allowing for finite experimental energy resolution, the calculations reproduce the observed behaviour quite well. In figure 2 the results obtained between 1 and 2 eV are shown while in figure 3 the same results are shown (but not to scale) on an expanded energy scale in order to show the detailed threshold behaviour. While they are strongly affected by it, the curves in figure 2 do not really represent the threshold behaviour, since this is confined to a region $\pm 0{\cdot}001$ eV of the threshold. The difference between the results plotted on the scale of figure 2 and the threshold behaviour is clear from comparison of the two figures.

Below 30°, a shallow dip about 0·1 eV wide is found just above the threshold, the minimum occurring at about 1·64 eV at 20°. At 20° the cross section has a flat maximum at about 1·4 eV and decreases with decreasing energy. This is contrary to observation. As θ is increased to 30° and 40° the dip above threshold vanishes and the calculated variation is similar to that observed; the threshold behaviour at these angles takes the form of a step. Around 50° the curve is rather smooth

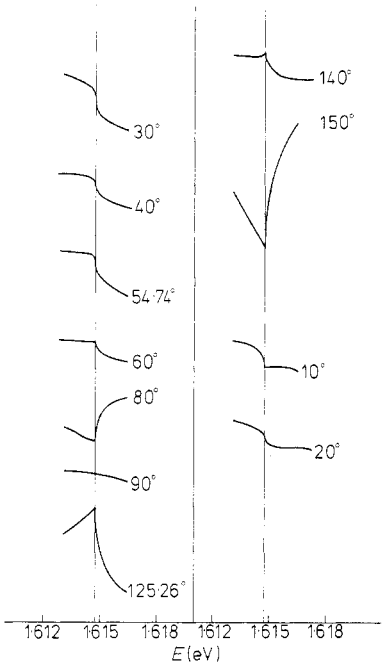

Figure 3. Cross sections (not to scale) of figure 2 in the immediate vicinity of the excitation threshold (1·61477 eV).

except for a tiny peak just below threshold (the maximum occurs at about 1·613 eV at 50°) followed by a flat cusp at the threshold, while at 60° the behaviour is similar except that the peak is flattened out and the cusp less marked. Both features are so small as to be scarcely observable on the scale chosen. By 80° the peak has gone and a tiny dip is obtained, which close examination reveals to be a downward cusp occurring at the threshold. At 90° the observed behaviour is reproduced very well near threshold, and so is the peak near 120° which is found to be indeed a cusp, exactly at the threshold. As the scattering angle is further increased the strong upward cusp is reduced and turns into a downward cusp, at threshold, above 145°.

This observed behaviour may be interpreted by examining the individual contributions to the total differential cross section. The angular variation of the cross section is clearly a result of the complicated interference of a number of partial waves. The cross section $\sigma(\theta)$ is given by

$$\sigma(\theta) = \tfrac{1}{4}|f^0(\theta)|^2 + \tfrac{3}{4}|f^1(\theta)|^2 \tag{4.1}$$

where $f^0(\theta)$ and $f^1(\theta)$ are respectively the singlet and triplet amplitudes defined by equation (2.1). Let us note that the triplet contribution has the higher weighting factor of 3; the $L = 0$ contribution is isotropic, since $P_0(\cos\theta) = 1$. The other partial-wave contributions will vanish at angles for which the appropriate Legendre polynomial $P_L(\cos\theta) = 0$, which for $L = 1$ is 90° and for $L = 2$, 54·74° and 125·26°. We also note that $P_L(\cos\theta) = (-1)^L P_L(\cos(\pi - \theta))$, so that where destructive interference occurs at a given angle, we might expect additive interference at its complement, and vice versa.

A number of partial waves contribute significantly to the sum, although at a fixed angle, the contribution from $L \geqslant 3$ is slowly varying. The explanation of the observed behaviour lies in the interference patterns produced between the S, P and D waves and the sum of the higher partial waves; and also in the relative contributions of the singlet and triplet parts. It cannot be said that any one partial wave determines the overall behaviour, although different partial waves tend to dominate as the scattering angle varies. Three factors however play an important role in determining the detailed structure; the broad ^{1}D resonance below threshold, the narrower ^{1}P resonance almost coincident with threshold, and the existence of the cusp effect in the P waves. As examination of the calculated T-matrix elements shows, this is very important in the ^{1}P wave owing to enhancement produced by the presence of the resonance; in the ^{3}P partial wave, although a cusp is there, it has an almost negligible effect.

At 30° the total triplet contribution, which varies slowly with energy, is about three times the singlet contribution. The ^{1}P part is rising and the ^{1}D falling, below the threshold, and this combination of effects produces the observed variation with energy. At 150°, destructive interference produces a much smaller cross section, and accounts for the drop below threshold which results in a downward cusp. The peak below threshold seen around 50° is due to the ^{1}P resonance. At this angle both a resonant peak and a cusp are observed, at slightly different energy. These features are, however, superimposed upon a large triplet background which has no resonant components and in which the P-wave cusp is insignificant. The result is that the structure is not very pronounced. This swamping out is even more apparent at 60° where the peak and cusp almost disappear. The effect is accentuated by destructive interference in the singlet part. At 120°, however, the triplet contribution is reduced drastically by destructive interference; at this angle the D-wave contributions are small and the cross section is dominated by the ^{1}P resonance. The total effect of all partial waves is to lead to a maximum, and hence a cusp, at the threshold.

The effect of the ^{1}P resonance may be isolated from D-wave interference by looking at the results at those angles where the $L = 2$ contribution vanishes. At 54·74° the cross section falls smoothly and rapidly, except for a small superimposed peak with its maximum just below the threshold. This is *not* a cusp, but rather a resonance in the ^{1}P wave. The form of the cross section resembles that of the photodetachment cross section, which might be expected, since the shape is determined mainly by the ^{1}P partial wave, albeit superimposed on a smooth background due to the triplet contribution. The 125·26° cross section is much reduced in magnitude because of destructive replacing additive interference. The shape is similar to that observed at 120° and its interpretation similar to that given for that case. Similarly, the effects of the D-wave on its own may be studied at 90° where the P wave and all other odd partial waves vanish. At 90°, the ^{1}D wave dominates the behaviour; a combination of the broad resonance below threshold and a rapid decrease above it, owing to loss of flux into the inelastic channel, produce the observed cross section. Note that in the absence of P waves the derivative is continuous at threshold (figure 3).

4.2. Elastic angular distributions

The previous section was devoted to a discussion of the behaviour of the fixed-angle elastic differential cross section as a function of energy in the vicinity of the excitation

threshold. In this section we discuss the angular dependence of the differential cross sections for fixed energy.

Unnormalized angular distributions of electrons elastically scattered by potassium atoms have been measured by McMillen (1934), at energies of 5 eV or above, and also by Gehenn and Wilmers (1971) between 0·9 and 15 eV. Using the 120° cusp for energy calibration, Eyb and Hofmann have repeated these measurements at 1·2 eV, with results in better agreement with the theory of Karule, and also at 2·2 eV. Collins *et al* (1971) have performed measurements at 0·5, 0·75, 1·0 and 1·2 eV, normalizing the results to their measured total cross section at 1·0 eV, 2×10^{-14} cm^2. Slevin *et al* (1972) have measured absolute differential cross sections both for elastic scattering and (above 1·61 eV) for excitation of the 4p state, at 1·0, 3·0, 4·4 and 5·2 eV at intermediate angles. Collins *et al* combine their measurements with a determination of the ratio $|g(\theta)|^2/\sigma(\theta)$ of the differential spin-flip to the total differential cross sections and are thus able to deduce the absolute value of the exchange amplitude, $|g(\theta)|$. A complementary experiment is that of Hils *et al* (1972) in which the ratio $|f(\theta)|^2/\sigma(\theta)$, where $f(\theta)$ is the direct amplitude, is measured by scattering 3·3 eV unpolarized electrons from polarized K atoms. Again, simultaneous measurement of $\sigma(\theta)$ enables $|f(\theta)|$ to be determined.

A selection of these results is illustrated in figure 4 and compared with theory. On the whole, our calculated angular distributions obtained below 1·61 eV are in good agreement with those calculated by Karule (1972). Typical of this agreement are the results at 1·6 eV (figure 4(*a*)), 1·0 eV (figure 4(*c*)) and 1·2 eV (figure 4(*d*)). The main differences occur in the forward direction, where the effects of including an infinite number of partial waves becomes apparent, and in the region of the minima, where the cross sections are small and depend sensitively on the interference of the differential partial waves. At 0·5 (figure 4(*a*)) and 0·75 eV (figure 4(*b*)) the calculated cross section is in quite good agreement with the experiment of Collins *et al* (1971) except near the minimum. (The experimental error is estimated by Collins *et al* to be $\pm 25\%$.) At 1·0 eV very good agreement with the absolute measurements of Slevin *et al* (1972) is obtained between 40° and 60°, as illustrated in figure 5 which utilizes a linear scale. Below 40° the experimental results fall below theory and are in better agreement with Karule (see figure 4(*c*)). The maximum error quoted by Slevin *et al* is 15%, and the angular uncertainties are shown in the figure. The results of Collins *et al* (1971) however (figure 4(*c*)) lie above and are in slightly better agreement with the present calculations below 40°, at this energy. At 1·2 eV (figure 4(*d*)) the present results and those of Karule are equal at 50°; if normalized to theory at this angle the relative measurements of Eyb and Hofmann are in better general agreement with the present calculations, in particular with regard to the position of the minimum. At this energy the results of Collins *et al* are in fair agreement but predict the minimum at about 105° instead of at about 120°. These results confirm the superiority of the results of Eyb and Hofmann over the earlier ones by Gehenn and Wilmers at $1{\cdot}1 \pm 0{\cdot}2$ eV (not illustrated). The ratio $|g|^2/\sigma$ is shown in figure 6, and compared with the calculation of Karule and experimental results of Collins *et al*. Agreement between theory and experiment is satisfactory if one takes into account the overall apparatus angular resolution which varies from about 60° (above 120°) to around 15° below 60°. Figure 7 shows the ratio $|g|^2/\sigma$ at 180° plotted against energy; agreement between all three sets of results is excellent.

In figure 8(*a*) are shown some results at 3 eV; the relative experimental points of Hils *et al* (at 3·3 eV) and those of Gehenn and Wilmers (at $3{\cdot}1 \pm 0{\cdot}3$ eV) and

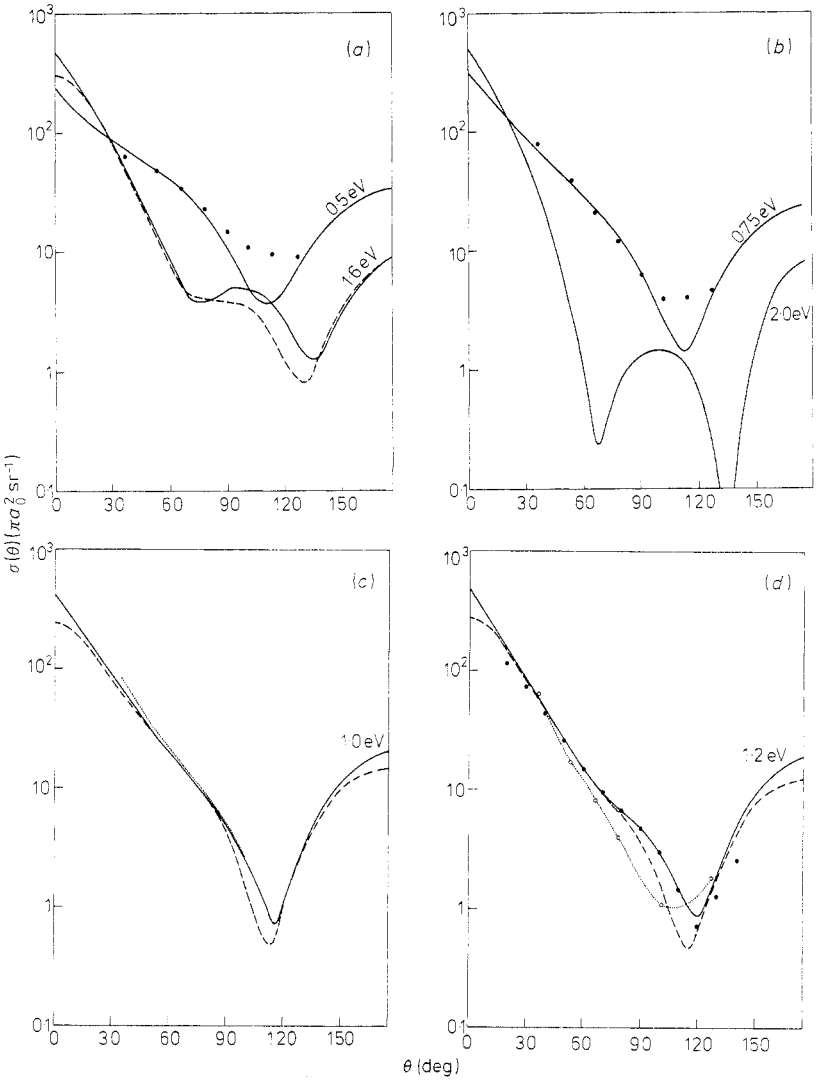

Figure 4. Differential cross sections for scattering of electrons by potassium atoms. (*a*) Present results (0·5 eV and 1·6 eV): full curves; Karule (1965) (1·6 eV): broken curve; Collins *et al* (1971) (0·5 eV); ●. (*b*) Present results (0·75 eV and 2·0 eV): full curve: Collins *et al* (1971) (0·75 eV): full circles. (*c*) Present results: full curve; Karule (1965): broken curve; Collins *et al* (1971): dotted curve. (*d*) Present results: full curve; Karule (1965): broken curve; Eyb and Hofmann (1974): full circles; Collins *et al* (1971): dotted curve with open circles.

the theoretical curve obtained from the calculation of Karule and Peterkop have all been normalized such that the secondary maximum occurs at 1·0 πa_0^2. The three-state close-coupling results are seen to be in better agreement, as regards shape, with these relative measurements than are the two-state results of Karule and Peterkop. The position of the minima are in much better accord, although the observed minimum near 60° is much deeper. The absolute measurement by Slevin *et al* is in rather poor agreement with theory, however. Some 5 eV results are shown in

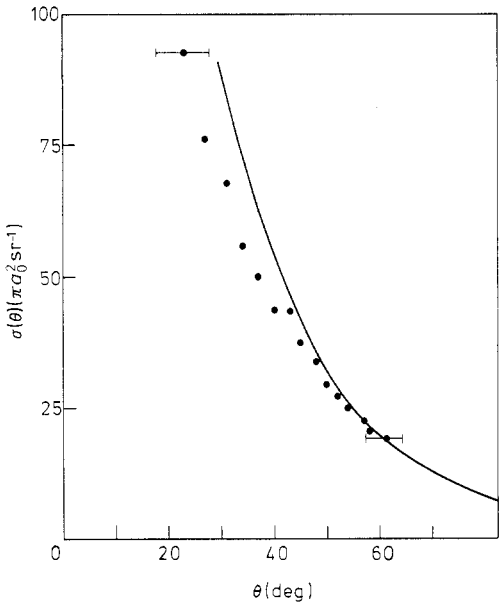

Figure 5. Differential cross section at 1·0 eV, on a linear scale. Present results: full curve; Slevin *et al* (1972): full circles.

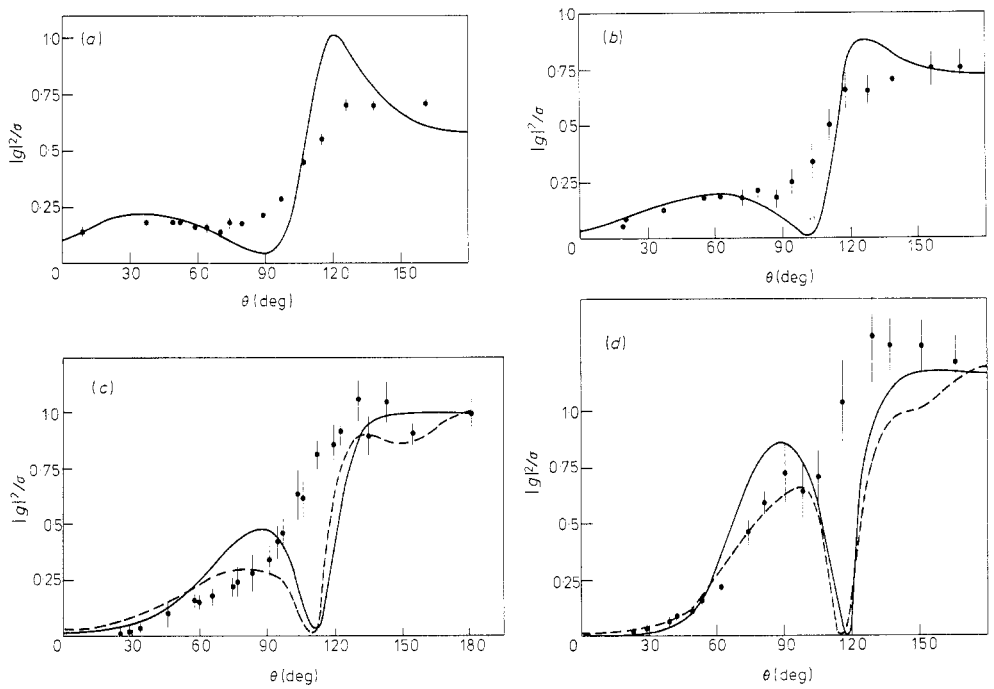

Figure 6. $|g|^2/\sigma$ plotted against θ. (*a*) 0·5 eV (*b*) 0·75 eV (*c*) 1·0 eV (*d*) 1·2 eV. Present results: full curves; Karule (1965): broken curves; Collins *et al* (1971): full circles.

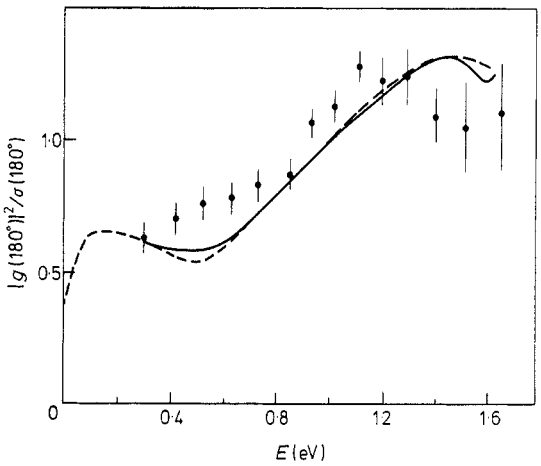

Figure 7. The ratio $|g|^2/\sigma$ at 180° as a function of energy. Symbols as in figure 6.

figure 8(*b*) together with the calculations of Karule and Peterkop, and the relative measurements of McMillen (1934) and of Gehenn and Wilmers (1971) (5·0 ± 0·5 eV) both normalized to our theory at 90°. The two theoretical curves are in quite good mutual agreement, and there is some evidence of a displacement of the observed

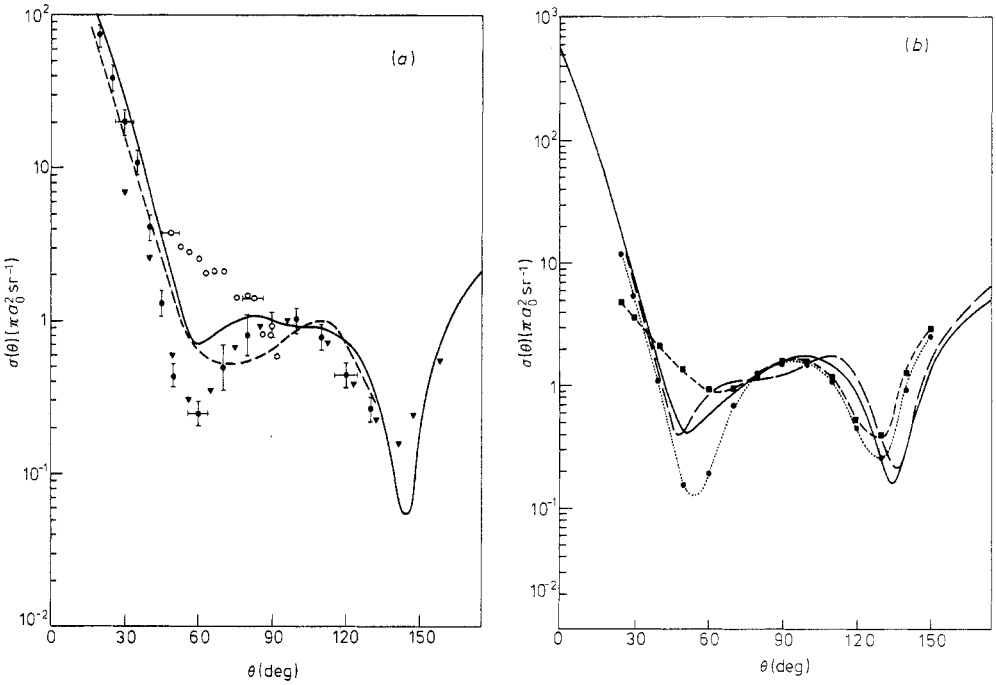

Figure 8. Differential cross section for elastic scattering of electrons by potassium atoms. (*a*) 3 eV. Present results: full curve; Karule and Peterkop (1965): broken curve; Gehenn and Wilmers (1971) at 3·1 ± 0·3 eV: ▼; Hils *et al* (1972) at 3·3 eV: ●; Slevin *et al* (1972): ○. (*b*) 5 eV. Present results: full curve; McMillen (1934): –■–; Gehenn and Wilmers (1971) (5·0 ± 0·5 eV): ···●···; Karule and Peterkop (1965): broken curve.

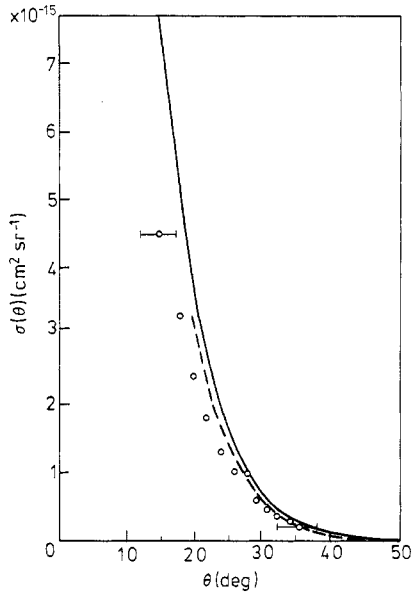

Figure 9. Differential cross section at 5 eV on a linear scale. Present results: full curve; Karule and Peterkop (1965): broken curve; Slevin *et al* (1972) (5·2 eV): open circles.

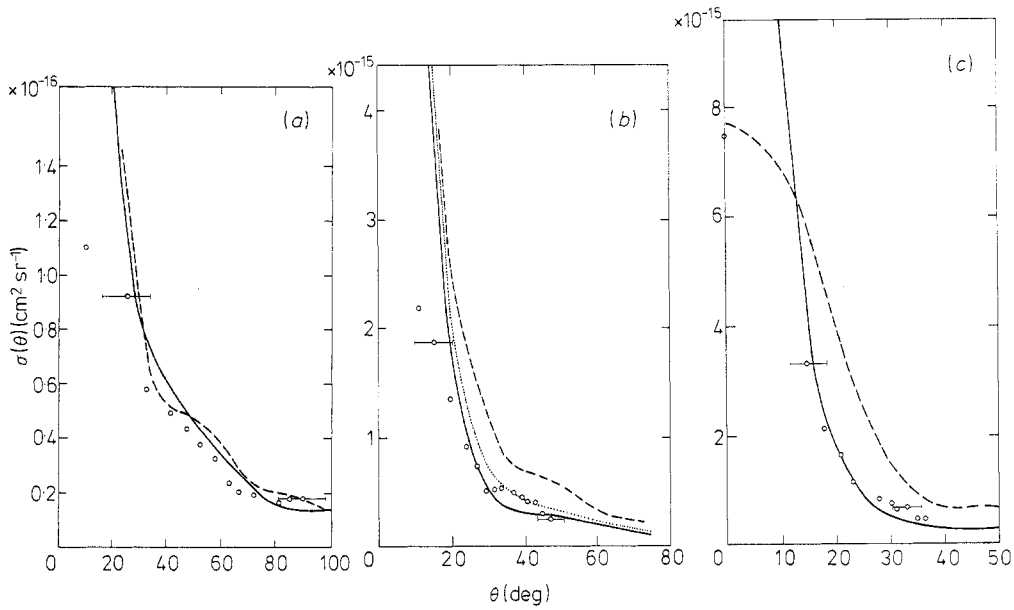

Figure 10. Differential cross section for excitation of the 4p state of potassium by electrons. (*a*) 3 eV. Present results: full curve; Karule and Peterkop (1965): broken curve; Slevin *et al* (1972): open circles. (*b*) Present results (5 eV): full curve; present results (4 eV): dotted curve; Karule and Peterkop (1965) (4 eV): broken curve; Slevin *et al* (1972) (4·4 eV): open circles. (*c*) Present results (5 eV): full curve; Karule and Peterkop (1965) (5 eV): broken curve; Slevin *et al* (1972) (5·2 eV): open circles.

minima with respect to theory. Otherwise, the picture is similar to that for 3 eV. In figure 9 we show the 5 eV results between 15° and 50° plotted on a linear scale and compared with the absolute measurements at 5·2 eV of Slevin *et al* who quote an uncertainty in the measured energy of ±0·15 eV and a maximum error in the cross section of 15%; the experimental angular uncertainty is shown in the figure. In this case agreement between theory and experiment is very good, especially when it is noted that the effect of increasing the energy of the calculation to the value at which the experiment was performed, 5·2 eV, would be to decrease the calculated cross section at these angles. This agreement contrasts with the disagreement with the results of the same experiment at 3 eV.

4.3. Excitation of the 4p state

4.3.1. Differential cross section. In figure 10 the differential cross sections for excitation of the 4p state are compared with the calculations of Karule and Peterkop and the absolute experimental results of Slevin *et al* (1972). At 3 eV (apart from one odd experimental point below 20°) all three sets of results are in good agreement. However figures 10(*b*) and 10(*c*) demonstrate that the present results display a much closer agreement with experiment at 4 and 5 eV than do those of Karule. At these energies, not only does the 3d state affect the results, but inclusion of high partial waves neglected by Karule and Peterkop is essential to ensure convergence of the excitation amplitudes, even though the effect on the integrated cross section may be small.

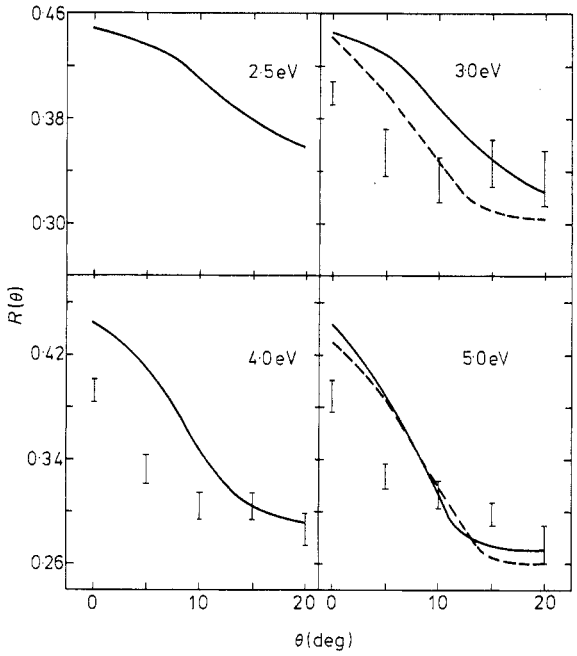

Figure 11. $R(\theta)$ plotted against θ. Present results: full curves; Karule and Peterkop (1965): broken curves; Goldstein *et al* (1972): I.

4.3.2. Recoil experiments. The recoil experiments of Rubin *et al* (1969) and Goldstein *et al* (1972) measure the ratio $R(\theta)$ of the relative number of atoms, initially spin polarized, which change their spin after excitation of the 4p state and subsequent radiative decay back to the 4s ground state, with the electrons scattered through an angle θ. In these experiments the electron energies range from the excitation threshold to 20 eV and the angle θ from 0 to 20°. Experimental and theoretical values obtained for this ratio are compared in figure 11. Goldstein *et al* quote an angular resolution of about 5°, but more than this for small energies and angles; if this is taken into account, one may say that theory and experiment are in good agreement with each other; and particularly so at 15° and 20°. The present results differ somewhat from those of Karule and Peterkop at 3 eV but not at 5 eV. The value obtained for $R(0)$ at the threshold was 0·51 compared with $0{\cdot}474 \pm 0{\cdot}014$ obtained by Rubin *et al*.

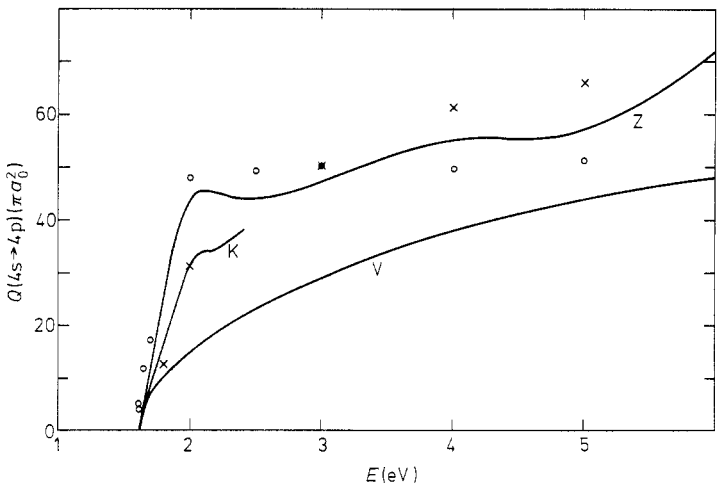

Figure 12. Total cross section for excitation of the 4p state of potassium by electron impact. Present results: ○; Karule and Peterkop (1965): ×; Vainshtein *et al* (1965): V; Korchevoi and Przonski (1967): K; Zapesochnyi and Shimon (1966): Z.

4.3.3. Total cross sections. The absolute, total cross section for excitation of the 4p state has been measured by Volkova and Devyatov (1963) and subsequently by Zapesochnyi and Shimon (1966) whose results are about a factor of two smaller at the maximum. Zapesochnyi and Shpenik (1966) in a relative measurement with improved energy resolution have observed local maxima at 2·1, 4·0 and between 10 and 12 eV. Korchevoi and Przonski (1967) have also obtained the 2·1 eV maximum, but their measured cross section is about 25% smaller than that obtained by Zapesochnyi and Shimon (1966). Some results are shown in figure 12. The present calculations are in better agreement with the Zapesochnyi and Shimon results than are the calculations of Karule and Peterkop, and are consistent with the existence of the observed maximum at 2·1 eV. This is due to resonant behaviour in the ^3F partial wave. The slope of the calculated cross section at threshold is much steeper than that predicted by Korchevoi and Przonski. The calculation of Vainshtein *et al* (1965) falls well below experiment at these energies. Other calculations not illustrated include those by McCavert and Rudge (1972) which display good agreement with Zapesochnyi

and Shimon (1966) above the 3d excitation threshold at 2·6 eV and the Glauber calculation of Walters (1973) which is in poor agreement with experiment below 5 eV as might be expected of a high-energy approximation, although much better than the Born result of Vainshtein *et al* (1965). The semi-classical results of Mathur *et al* (1969) are likewise in poor agreement with experiment. The agreement between the present result and the measurement of Zapesochnyi and Shimon contrasts with the situation found in excitation of the resonance transitions of lithium (Leep and Gallaher 1974) and sodium (Moores and Norcross 1972) where the results of Zapesochnyi and collaborators lie a factor of about two below the close-coupling calculations, which however are in agreement with more recent experimental work. At the same time it should be noted that Smith (Moiseiwitsch and Smith 1968) has pointed out an error in the interpretation of the results of Zapesochnyi *et al* for sodium (and possibly for the other alkali metals as well) which, if corrected, would scale up the cross sections by a factor of 1·6 and so bring the lithium and sodium results into agreement with the other work. The potassium results however if scaled in such a way would then lie well above the close-coupling calculations.

5. Total scattering

The absolute total cross section measurements of Brode (1929), carried out using a modified Ramsauer-type apparatus, have since been repeated by Collins *et al* (1971) and by Visconti *et al* (1971) using an atom-beam recoil technique. As in the case of the other alkali metals, the results of these more recent measurements are in substantial disagreement with those of Brode, but are in good agreement with the theoretical results of Karule (1965) and Karule and Peterkop (1965). The measurements have been extended up to 50 eV by Kasdan *et al* (1973).

Total scattering and spin-flip cross sections are shown in figure 13. Below the excitation threshold our results are about 10% larger than those of Karule, and are hence in less good agreement with the experiment. Since the overall error in the measured cross section of Visconti *et al* is estimated to be $\pm 10\%$ our results are still consistent with experiment. The sudden small drop at threshold, observed by Eyb and Hofmann, is also obtained in our calculated cross section.

Above the threshold, the sum of the elastic and 4s–4p excitation cross sections falls below the results of Karule and Peterkop at around 2·5 eV and is again in less good agreement with the measured cross section (which however contains contributions from all inelastic $s \rightarrow p$ processes). Total spin-flip cross sections have been measured by Collins *et al* (1971) and by Campbell *et al* (1971), the latter results at 1 eV being about a factor of two larger than the former. Except in the region of the excitation threshold, the calculated cross sections are in good agreement with the results of Karule which are in fair agreement with Collins *et al*, just falling within the upper limit of their error bars. A small peak is obtained at the excitation threshold due partly to the resonances below threshold and partly to the onset of excitation. Above threshold the calculated cross section (sum of elastic and $4s \rightarrow 4p$ contributions) shows better agreement with Campbell *et al* whose results also contain an unknown contribution from other inelastic spin-flip processes and thus might be expected to be a bit larger than theory. The total cross section data are collected in table 3. Below the excitation threshold we tabulate the total, spin-flip and momentum transfer cross sections, all for elastic scattering; above it, the same cross sections

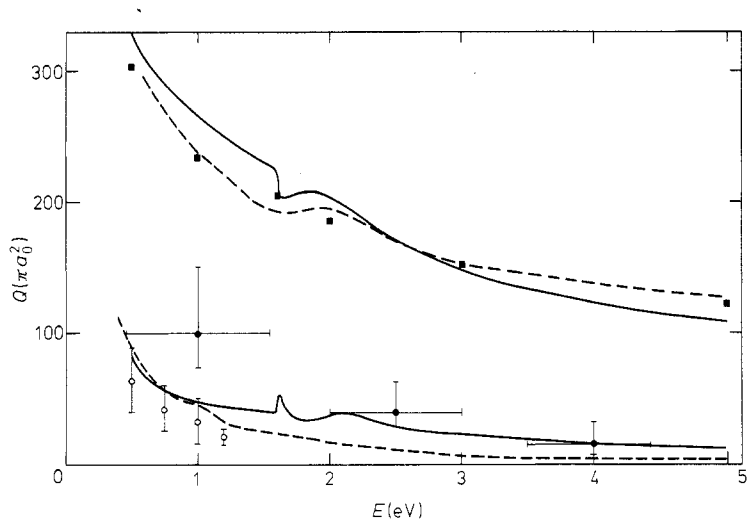

Figure 13. *Upper Curves.* Total cross section for e^-–K scattering. Visconti *et al* (1972): ■; Karule (1965) and Karule and Peterkop (1965): broken curve; present results: full curve. Theoretical curves are sum of elastic and 4s–4p excitation cross section. *Lower Curves.* Total spin-flip cross section. Collins *et al* (1971): ϕ; Campbell *et al* (1971): ⊕; present results: full curve; Karule (1965) and Karule and Peterkop (1965) (elastic only): broken curve.

but for 4s → 4p excitation are given in addition, together with the integrated amplitudes D_M, E_M and I_M defined by Moores and Norcross (1972) (equation (2.26)) which refer to excitation of the magnetic sublevels of the 4p state. The only quantity above not defined by Moores and Norcross is the momentum transfer (or diffusion) cross section for 4s → 4p excitation which is obtained from

$$\sigma_D(4s \rightarrow 4p) = \frac{k_f}{k_i} \sum_{S=0,1} \frac{2S+1}{4} \sum_{M=0,\pm 1} \int |f_M^S(\theta, \phi)|^2 (1 - \cos\theta) \sin\theta \, d\theta \, d\phi$$

where $f_M^s(\theta,\phi)$ is the excitation amplitude for magnetic sublevel M and total spin S.

6. Conclusions

The comparison of the computed phaseshifts (§ 3.1) and the degree of accord obtained between the present three-state calculations and the two-state results of Karule (1965), both for the elastic differential cross section $\sigma(\theta)$ and for $|g|^2/\sigma$ (illustrated in figures 4–7), point to the conclusion that at least for elastic scattering below about 1·6 eV, the three-state results do not differ from the two-state results to an extent sufficient to justify the considerable amount of extra work that they entail. Both calculations show good agreement with the experimental results of Collins *et al* (1971) and Slevin *et al* (1972) when the experimental error limits are taken into account. Where any major differences exist between the calculations they may be attributed to higher partial waves neglected in Karule's calculation.

The effects of the 3d state begin to play a role in determining the details of the scattering above 1·6 eV. A three-state calculation at least is necessary to predict

Table 3. Total cross sections in units of πa_0^2.

E(eV)	$Q(4s \rightarrow 4s)$	$Q_{ST}(4s \rightarrow 4s)$	$Q_D(4s \rightarrow 4s)$	$Q(4s \rightarrow 4p)$	$Q_{ST}(4s \rightarrow 4p)$	$Q_D(4s \rightarrow 4p)$
0·5	375·2	94·6	208·2			
0·75	329·3	64·6	142·5			
1·0	302·0	52·9	109·4			
1·1	293·0	50·7	100·8			
1·2	284·5	49·2	93·6			
1·5	261·3	45·0	75·9			
1·6	254·6	44·6	68·2			
1·6131	249·8	50·4	65·5			
1·6140	248·3	52·3	65·2			
1·6155	238·0	53·0	62·5	4·1	5·0	4·3
1·6165	236·0	51·7	61·8	5·0	6·2	5·6
1·65	219·1	37·5	50·1	11·8	12·7	15·1
1·7	213·6	26·4	40·8	16·9	15·8	19·4
2·0	182·5	17·9	30·4	47·9	22·6	48·2
2·5	143·9	10·9	21·6	49·2	20·3	34·3
3·0	114·4	7·5	14·9	50·0	16·8	26·0
4·0	88·5	5·3	15·0	49·7	10·8	15·4
5·0	73·9	3·9	17·3	51·1	7·7	11·3

E(eV)	D_0	E_0	I_0	D_1	E_1	I_1
1·6155	2·75	4·95	0·38	0·0041	0·0044	0·0002
1·6165	3·40	6·17	0·44	0·015	0·015	0·0007
1·65	8·09	10·7	0·65	1·01	0·96	0·085
1·7	10·8	12·2	1·99	2·05	1·78	0·50
2·0	20·0	19·3	29·4	4·72	1·66	7·17
2·5	21·0	17·1	29·9	6·87	1·58	6·71
3·0	20·2	13·8	29·8	8·04	1·47	8·58
4·0	19·8	8·56	27·2	9·85	1·14	10·9
5·0	19·8	5·59	25·3	11·5	1·07	13·2

the sharp ^{1}P resonance just below the excitation threshold. The details of the threshold behaviour of $\sigma(\theta)$ observed by Eyb and Hofmann may then be satisfactorily explained from the interference effects of the various partial waves and the relative strengths of triplet and singlet contributions. Only the slope of the 20° curve below 1·5 eV is an outstanding source of discrepancy between theory and this experiment. However, even above the excitation threshold and up to 5 eV the elastic differential cross section is not seriously changed by adding the 3d state, as comparison of the present results and those of Karule shows. Above 3·0 eV, on the other hand, the three-state results for the differential 4s → 4p excitation cross section differ significantly from those of Karule but are in quite good agreement with the experimental results of Slevin *et al.* The elastic differential cross sections are also in quite good agreement with Slevin *et al* except at 3 eV, where the results of Slevin *et al* differ considerably from theory and also differ qualitatively from the relative measurements of Gehenn and Wilmers and the results of Hils *et al* which are both in quite good agreement with theory. A second source of discrepancy is thus the 3 eV elastic scattering data of Slevin *et al* which disagree with the three-state calculation while at the

same time all the differential cross sections, elastic and inelastic at all other energies, agree with the results of the same calculation.

The three-state close-coupling approximation is capable of giving good agreement with the results of the recoil experiment of Goldstein *et al* (1972) at angles greater than 10° where the experimental angular resolution is not too bad, and also with the (uncorrected) total excitation cross section measured by Zapesochnyi and Shimon (1966). For inelastic processes the three-state calculation is an improvement over the two-state calculation of Karule and Peterkop. The total cross section is in less good agreement with Visconti *et al* than are the calculations by Karule, but is still within the experimental uncertainty; the structure near the excitation threshold observed by Eyb and Hofmann has also been obtained.

In summary, then, reasonable agreement between observed and calculated elastic scattering cross sections may be obtained without recourse to a method more elaborate than a two-state 4s–4p close-coupling approximation. This indicates that the chief mechanism affecting the elastic scattering of slow electrons by potassium atoms is the long-range potential behaving asymptotically like r^{-2} which strongly couples the 4s and 4p states and which contributes most of the dipole polarizability of the atom. Inclusion of the 3d state is required to reproduce the finer details observed in some of the experiments such as the behaviour of the elastic differential cross sections near the first excitation threshold, to locate accurately the positions of resonances, and to improve results of calculations involving excitation of the 4p state. If cross sections for transitions between excited states were required, however, it is unlikely that such a simple approximation would be adequate and for these processes it would no doubt be very important to include coupling to higher excited states in the expansion.

The effects on the elastic scattering phaseshifts (figure 1) (below about 1·6 eV) of including the 3d state in the expansion are of about the same magnitude as uncertainties due to the use of alternative target wavefunctions. Future calculations should concentrate as much on a more accurate representation of the target as upon inclusion of more of the interaction between the target and the electron. For atoms as large as potassium, the concept of a core of closed shells is beginning to lose its validity, and it is doubtful if the approximation of replacing the core by a central potential of the form used in the present work is as good as it is in the case of, say, sodium. Apart from this, direct and exchange terms arising from the dipole moment induced in the core by one electron influencing the motion of the other electron (the 'dielectric effects') should be included in the scattering problem. It is also possible that the explicit inclusion of spin–orbit terms in the interaction Hamiltonian could be important during the collision process.

Acknowledgments

The computer program used in this work was developed jointly by the author and by Dr D W Norcross, of the Joint Institute for Laboratory Astrophysics, Boulder, Colorado, and is partly an adaptation of a code originally supplied by Professor P G Burke to the author. Dr Norcross must also be thanked for providing a number of references to experimental work on excitation and for various comments.

References

Andrick D, Eyb M and Hofmann H 1972 *J. Phys. B: Atom. Molec. Phys.* **5** L15–7
Brode R B 1929 *Phys. Rev.* **34** 673–8
Campbell D M, Brash H M and Farago P S 1971 *Phys. Lett.* **36A** 449–50
Collins R E. Bederson B and Goldstein M 1971 *Phys. Rev.* A **3** 1976–87
Eminyan M, MacAdam K B, Slevin J and Kleinpoppen H 1974 *J. Phys. B: Atom. Molec. Phys.* **7** 1519–42
Eyb M and Hofmann H 1975 *J. Phys. B: Atom. Molec. Phys.* **8** 1095–1108
Fano U and Macek J H 1973 *Rev. Mod. Phys.* **45** 553–73
Gaspar R 1952 *Acta Phys. Acad. Sci. Hung.* **2** 151–9
Gehenn W and Wilmers M 1971 *Z. Phys.* **244** 395–401
Goldstein M, Kasdan A and Bederson B 1972 *Phys. Rev.* A **5** 660–8
Hahn Y, O'Malley T F and Spruch L 1964 *Phys. Rev.* **134** B911–8
Hertel I V and Stoll W 1974 *J. Phys. B: Atom. Molec. Phys.* **7** 570–92
Hils D, McCusker M V, Kleinpoppen H and Smith S J 1972 *Phys. Rev. Lett.* **29** 398–401
Karule E M 1965 *Atomic Collisions III* ed V Ia Veldre (Riga: Latvian Academy of Science) (Translation TT66-12939 available through SLA Translation Center, Chicago)
Karule E M 1972 *J. Phys. B: Atom. Molec. Phys.* **5** 2051–60
Karule E M and Peterkop R K 1965 *Atomic Collisions III* ed V Ia Veldre (Riga: Latvian Academy of Science) (Translation TT 66-12939 available through SLA Translation Center, Chicago)
Kasdan A, Miller T M and Bederson B 1973 *Phys. Rev.* A **8** 1562–9
Korchevoi Yu P and Przonski A M 1967 *Sov. Phys.–JETP* **24** 1089–92
Leep D and Gallaher A 1974 *Phys. Rev.* A **10** 1082–90
Mathur K C, Tripathi A N and Joshi S K 1969 *J. Chem. Phys.* **50** 2980–3
McCavert P and Rudge M R H 1972 *J. Phys. B: Atom. Molec. Phys.* **5** 508–13
McMillen J H 1934 *Phys. Rev.* **46** 983–8
Moiseiwitsch B L and Smith S J 1968 *Rev. Mod. Phys.* **40** 238–353
Moores D L and Norcross D W 1972 *J. Phys. B: Atom. Molec. Phys.* **5** 1482–505
——1974 *Phys. Rev.* A **10** 1646–57
Norcross D W 1971 *J. Phys. B: Atom. Molec. Phys.* **4** 1458–75
——1974 *Phys. Rev. Lett.* **32** 192–5
Norcross D W and Seaton M J 1973 *J. Phys. B: Atom. Molec. Phys.* **6** 614–21
Rubin K, Bederson B, Goldstein M and Collins R E 1969 *Phys. Rev.* **182** 201–14
Seaton M J 1961 *Proc. Phys. Soc.* **77** 174–83
Sinfailam A L and Nesbet R K 1973 *Phys. Rev.* A **7** 1987–94
Slevin J A, Visconti P J and Rubin P J 1972 *Phys. Rev.* A **5** 2065–77
Vainshtein L A, Opykhtiu V and Presnyakov L 1965 *Sov. Phys.–JETP* **20** 1542–5
Visconti P J, Slevin J A and Rubin K 1971 *Phys. Rev.* A **3** 1310–7
Volkova L M and Devyatov A 1963 *Bull. Acad. Sci. USSR Phys. Ser.* **27** 1025–8
Walters H R J 1973 *J. Phys. B: Atom. Molec. Phys.* **6** 1003–19
Zapesochnyi I P and Shimon L L 1966 *Opt. Spectrosc.* **21** 155–7
Zapesochnyi I P and Shpenik O B 1966 *Sov. Phys.–JETP* **23** 592–6